Durham University

Durham Research Online

Deposited in DRO:

14 April 2009

Version of attached file:

Accepted Version

Peer-review status of attached file:

Peer-reviewed

Citation for published item:

Bailiff, I. K. and Mikhailik, V. B. (2003) 'Spatially-resolved measurement of optically stimulated luminescence and time-resolved luminescence.', Radiation measurements., 37 (2). pp. 151-159.

Further information on publisher's website:

http://dx.doi.org/10.1016/S1350-4487(02)00187-7

Publisher's copyright statement:

Additional information:

Use policy

The full-text may be used and/or reproduced, and given to third parties in any format or medium, without prior permission or charge, for personal research or study, educational, or not-for-profit purposes provided that:

- a full bibliographic reference is made to the original source
- a link is made to the metadata record in DRO
- the full-text is not changed in any way

The full-text must not be sold in any format or medium without the formal permission of the copyright holders.

Please consult the full DRO policy for further details.

Durham University Library, Stockton Road, Durham DH1 3LY, United Kingdom
Tel : +44 (0)191 334 3042 | Fax : +44 (0)191 334 2971
https://dro.dur.ac.uk

Spatially-resolved measurement of optically stimulated luminescence and time-resolved luminescence

I.K.Bailiff* and V.B.Mikhailik

Luminescence Dosimetry Laboratory, Environmental Research Centre, Dawson Building,
University of Durham, South Road,
Durham DH1 3LE, UK

Abstract

Spatially-resolved measurements of optically stimulated luminescence (OSL) were performed using a two dimensional scanning system designed for use with planar samples. The scanning system employs a focused laser beam to stimulate a selected area of the sample, which is moved under the beam by a motorised stage. Exposure of the sample is controlled by an electronic shutter. Mapping of the distribution of OSL using a CW laser source was obtained with sub-millimeter resolution for samples of sliced brick, synthetic single crystal quartz, concrete and dental ceramic. These revealed sporadic emission in the case of brick or concrete and significant spatial variation of emission for quartz and dental ceramic slices. Determinations of absorbed dose were performed for quartz grains within a slice of modern brick. Reconfiguration of the scanner with a pulsed laser source enabled quartz and feldspathic minerals within a ceramic sample to be differentiated using a single stimulation wavelength by measuring the time-resolved luminescence spectrum.

Keywords: optically stimulated luminescence, spatially-resolved OSL, time-resolved luminescence, retrospective dosimetry, polymineral samples

*Corresponding author:
e-mail: Ian.Bailiff@durham.ac.uk, fax: 44-0191-374-3619; phone: 44-0191-374-3624

Acknowledgements

The work described in this paper was supported by the University of Durham and the European Commission within its 5th Framework Programme (1998-2002), Nuclear Fission and Radiation Protection, under Contract N° FIGD-CT-2000-00094. The latter is a collaborative project with: Ciemat, Madrid, GSF Neuherberg, Risø National Laboratory and the University of Helsinki. Earlier financial support by the NERC (grantss GR3/9568 and GST/02/0756) for development of a prototype scanning system is also acknowledged. We are grateful to Dr. R. Clark for programming, Dr. S. Chyriwsky for assistance in developing the prototype scanner and Mr. S. Grainger for technical assistance in sample preparation. We are grateful to Landauer Inc. for donation of Al_2O_3:C dosemeter powder.

1. Introduction

The determination of absorbed dose by measurement of the integrated luminescence, stimulated either thermally or optically, forms the basis of the commonly used techniques in luminescence dating and dosimetry. The success of such determinations is critically dependent on the ability of the mineral stimulated to yield sufficient luminescence, and it is well known that the sensitivity of minerals found in typical samples may vary by orders of magnitude between not only different mineral types but also the same mineral (e.g. quartz). This is in contrast to synthetic luminescent phosphors, such as those used for dosimetry and imaging, that are manufactured to be homogeneous. In the case of the latter, for example, storage phosphors on image plate detectors are used to determine the spatial distribution of ionising radiation (Thoms and von Seggern, 1996). In dating and retrospective dosimetry studies, typical samples are likely to contain a heterogeneous distribution of minerals possessing different sensitivity and dose histories, and the latter presents particular difficulties in the case of unheated sediments. The separation and isolation of a particular mineral component for luminescence measurements, which requires the fragmentation of the sample matrix, has consequently formed a key part of the development of routine techniques for absorbed dose determination. The use of spatially-resolved detectors has revealed that variations between grains of the same mineral type commonly occur due to differing sensitivity (heated and sediment samples) and differing dose histories (sediment samples), and both can lead to complications in absorbed dose evaluation. Several different forms of detection system capable of spatially-resolved measurement of either optically or thermally stimulated luminescence have been reported in the literature, including: image intensifiers (Templer and Walton, 1983; Huntley and Kirkey, 1985), photographic films (Hashimoto *et al.*, 1989; Hashimoto *et al.*, 1995), imaging photon detectors (Smith *et al.*, 1991; McFee and Tite, 1994) and CCD-cameras (e.g. Hashimoto *et al.*, 1995, Duller *et al.*, 1997; Spooner, 2000; Greilich *et al.*, 2002). Although the latest CCD-cameras are claimed to offer high

spatial resolution (~10 μm), wide spectral sensitivity and high quantum efficiency, the overall sensitivity of these systems still appears to be inferior to PMT-based readers. This is largely due to a lower signal-to-noise ratio and the reported levels of minimal detectable absorbed dose are several Gy for samples of K-feldspar (grains, Duller *et al.*, 1997; slices, Greilich *et al.*, 2002).

Another approach that can be used to perform spatially-resolved measurement of OSL is based on the use of a focused laser beam to stimulate a selected area of sample and to detect the luminescence using a single PMT. By moving the beam across the sample or by moving a sample under a fixed beam, executing a scanning action, spatially-resolved measurement of the luminescence can be performed by appropriate control of the photon detection system. This approach was applied to measure optically stimulated luminescence (OSL) from storage phosphor plates used in radiographic systems (Blasse and Grabmaier, 1994), and a one-dimensional OSL scanning system was used by Bøtter-Jensen *et al.* (1995) to record depth-dose profiles in ceramic materials. The development of a two dimensional OSL scanning system for use with planar ceramic samples was demonstrated by Bailiff *et al.* (1996), and similar elements of this approach were employed by Duller *et al.* (1999; 2000) in the development of an automated scanning system. The latter enables OSL measurements to be performed with separated single-grains, where the laser beam is moved discretely to each grain in a 9×9 location grid. In this paper we describe a two-dimensional scanning system that is based on the prototype (Bailiff *et al. loc. cit*) and which can perform measurement of the OSL signal from slices (and grains) with a sub-millimeter resolution. The scanner has been configured to map the distribution of OSL and to perform *in situ* determinations of absorbed dose for grains within a sample matrix (e.g. a ceramic slice). The scanner is used with either a

continuous wave (CW) or a pulsed laser stimulation source, the latter being used to investigate the mineral type by measuring time-resolved luminescence (TRL).

2. Instrumentation

A schematic diagram of the OSL scanner is shown in Fig. 1; the assembly is contained within a light-tight housing. The central component of the apparatus comprises a motorized X-Y stage (Physik Instrumente type C-832) on which a sample mount is located. The laser beam is directed onto the sample surface at angle of approximately 45º after passing through an electronically controlled shutter, a cut-off filter (to eliminate residual emission of laser pump radiation), neutral density filters selected to vary the stimulation intensity, a long-focus lens, and finally a front-surfaced mirror. The detection system, mounted 30 mm directly above the sample, comprises a PMT and optical filter system. The beam geometry was adjusted to prevent the reflected beam striking the detector. The specification of the detection system differs when using either the CW or pulsed laser sources and these are discussed further below. The sample is moved under the path of the beam in a stepwise manner under the PC control; after each increment the shutter is opened for a selected stimulation period (e.g. 200 ms) and the OSL recorded. In terms of scan images presented below the scan starts at the origin and proceeds in a raster pattern finishing at the top right corner of the image. Unless specified otherwise, an increment of 250 μm was selected for the measurements described in this paper, resulting in 1600 measurement points per complete scan. Once started, a scan is performed under software control and takes about 30 mins to complete, most of the time being required for stage movement (~1 s per increment).

Depending on the nature of the experiment, CW or pulsed laser stimulation was used. The constant intensity source comprised a CW Ar-ion laser (Reliant 250D, Laser Physics),

operated in multi-lines mode. When using this source the detection system comprised an EMI 9635QA PMT and Schott U-340 filters (6 mm), and the signal was fed to an Ortec ACE-MCS. Pulsed stimulation was provided by a tuneable optical parametric oscillator (Quanta Ray MOPO 710) pumped by a Q-switched YAG:Nd laser. The luminescence detection system is a further development of that described by Clark *et al.* (1997) and includes a fast PMT (EMI 9813QA) and a 2 ns resolution multi-channel scaler (Fast Comtec P7885) that enables the measurement of time-resolved luminescence. Two stimulation wavelengths were used with the pulsed source, either 500 or 850 nm, and the TRL was recorded using Schott U-340 (6 mm) and Schott BG-39 (3 mm) filters in the detection system respectively.

The optical system focuses the laser beam to a spot, the size of which is adjusted to suit the experiment and measured by use of a photodiode detector and a 50 μm-slit translated across the focal plane. Using the CW source, the beam diameter was adjusted to 250 μm and the incident power density set to either 1.5 or 3.6 W cm^{-2} using appropriate neutral density filters. The lower intensity was used to 'scan' the general OSL distribution with reduced trapped charge depletion.

To obtain precise sample re-positioning, samples (either sliced or granular) were fastened to machined metal plates. Good positioning accuracy of these plates was achieved using an adapted spring-loaded corner positioning stage originally manufactured for an optical microscope; positioning tests showed that the maximum deviation in positioning was about 30 μm. This was considered satisfactory given that the spatial resolution of the system is mainly determined by the beam diameter (set at 250 μm). Repeated experiments, which included several sample changes followed by scanning, showed no detectable lateral shift of the OSL image.

The control software allows the stage to move to a selected position within the scanned area so that an OSL decay curve can be recorded; this facility was employed when measuring CW OSL decay curves and the TRL spectra. A high precision diamond impregnated cutting wheel was used to produce slices of known and reproducible thickness (generally less than 1 mm). Absorbed doses were administered to samples using a beta irradiator containing a $^{90}Sr/^{90}Y$ β source, that had been previously calibrated against a ^{137}Cs photon source for granular samples (Göksu *et al.*, 1995); a further calibration experiment was performed to determine the absorbed dose for sliced ceramic samples. The dose-rate delivered by the laboratory source to 1 mm thick ceramic slices mounted on stainless-steel discs was 0.95 ±0.02 Gy min^{-1}.

3. Applications

3.1. OSL mapping

To illustrate the use of the equipment we include the results of measurements with ceramic samples (bricks) collected for retrospective dosimetry measurements, where the levels of absorbed dose are typically up to several hundred mGy. Examples of other heated and unheated materials, including annealed single crystal quartz, were also tested since the range of potential use clearly extends beyond ceramics. For the selection of brick samples tested so far and using standard OSL measurement procedures, the detected OSL was found in all cases to be concentrated in a few localised 'spots' within the 10 x 10 mm scanned areas, and the remainder of the cut surface yielded signals that were not significantly above the detector background. In the example shown in Fig. 2 OSL decay curves were only measurable at the 'spots' labelled A, and B the decay curves for which are shown in insets a and b. Subsequent examination of the slices under an optical microscope confirmed that the low number of

emitting spots was not due to a paucity of granular quartz or infrequent exposure of grains at the cut surface. These observations are consistent with past (Huntley and Kirkey, 1985) and recent findings (e.g. Duller *et al.*, 2000) that have revealed significant variations in the sensitivity of single grains for different types of sedimentary quartz.

Cementitious materials are also potentially useful for the retrospective dosimetry (Göksu *et al.*, 2002). An OSL scan performed with a slice of modern concrete (Fig. 3) reveals a very irregular distribution of OSL and the dynamic range of the detected signal is significantly higher than that found with brick. The dynamic range is due to the geological dose associated with the blend of minerals contained in the matrix; unfortunately the hydrated cement yields comparatively weak luminescence (Göksu *et al.*, 2002). Although differences in the rate of decay are likely to occur due to variations in the optical conditions within grains, the OSL decay curves show differences (Fig. 3, insets a and b) that may reflect mineral type (McKeever *et al.,* 1997), curves a and b being indicative of feldspar and quartz respectively. While tentative identification of the mineral species may be feasible based on decay rates, time resolved measurements can provide a more specific marker, as discussed at a later stage in this paper.

Dental porcelain, a ceramic of semi-vitreous composition that is of interest in retrospective dosimetry (Bailiff *et al.*, 2002a), was also examined. The measurement of spatially resolved OSL is of interest since it potentially offers the opportunity to select a particular mineral phase, if required, and also to measure a depth-dose profile where external beta particles and soft x-rays contribute to the external dose. Fig. 4 shows the spatial variation of the OSL for two slices of prosthetic tooth (i.e. solid dental porcelain) that were cut perpendicular to the main axis of the tooth, providing a horizontal cross section, measured immediately following

the administration of a beta dose and pre-heating. It is interesting to note that the OSL intensity decreases rapidly moving from the tooth core to the surface. Although there is a slight drop in beta dose with distance from the central axis, this is not attributed to the radial dependence of source dose rate. When originally calibrated, our source produced results similar to those published recently by Spooner and Allsop (2000), with a difference between centre and the edge of a 10 mm diameter sample of less than 10%. The observed change in OSL intensity is likely to reflect changes in sample sensitivity and reflects a layered structure resulting from the manufacturing process. This will be of importance in the study of optical and athermal fading effects that are currently under investigation (Bailiff *et al.*, 2002a).

Experiments were undertaken to test the capability of the scanner to measure absorbed dose as a function of depth in samples subjected to β- irradiation. The surface of a (thick) fragment of domestic porcelain was irradiated using a beta source (estimated sub-surface beta dose, 3 Gy). The fragment was subsequently cut in a direction perpendicular to the surface to provide a slice that extended from the surface glaze to the interior. The OSL map obtained for the slice is shown in Fig. 5 and, as found by Poolton *et al.* (1995), the OSL sensitivity of the glaze is significantly higher (attributed to the presence of Al_2O_3) than that of the interior matrix that appears to have negligible sensitivity. The OSL map from the glaze corresponds well to the spatial dimensions of the semi-transparent 250 μm thick glaze layer (Fig. 5). A similar experiment was performed with a 6 mm thick cylindrical pellet (diameter 10 mm) that was fabricated by combining granular Al_2O_3:C (Landauer Inc., 90-150 μm) with a setting binder. The pellet was irradiated using the laboratory β-source, delivering an absorbed dose of approximately 800 mGy in the sub-surface material. Slices were cut from the pellet along the axis of the cylinder to enable the depth-dose profile to be measured. The recorded distribution of the OSL (Fig. 6) shows a steep build-up at the edge and gradual decline to background

levels at about 4 mm below the surface. The general form of the OSL profile agrees well with that expected by calculation (Attix, 1986) and is consistent with a penetration depth of 3.8 mm estimated for β–particles in Al_2O_3 using the continuous slowing down approximation range (CSDA range, 1.51 g cm^{-2}; ICRU Report, 1984). Further calculation of the dose profile based on Monte Carlo simulation of electron transport is to be performed to enable a quantitative comparison of profiles to be obtained.

An OSL scanning system of the type described here, when compared with a spatially-resolved detector system that employs uniform stimulation across the sample, is expected to be at a disadvantage when measuring transparent or semi-transparent samples. The effects of optical scattering may reduce the effective spatial resolution of scanning due to the stimulation of a volume within which many single grains may be located. In this respect, the opacity of a clay-based ceramic matrix provides an important reduction in the level of light scattering between grains. Although a quantitative test to evaluate the extent of these effects in transparent slices has yet to be performed, we examined slices of synthetic quartz to explore the distribution of OSL. Slices of 1 mm thickness were cut (orthogonal to the z-axis) from a single bar of synthetic quartz (Sawyer Premium Q grade; see Petrov and Bailiff, 1995), polished and annealed at 1000 °C in air. The OSL map obtained with a beta-irradiated slice is shown in Fig. 7a and b. The distribution of OSL is very inhomogeneous, containing identifiable areas that emit relatively bright luminescence, and with a dynamic range of intensity that extends to an order of magnitude within the scanned area. Apart from the issue of spatial resolution achieved, the data indicate that the traps are spatially localized on a macroscopic scale, probably reflecting features of crystal formation during hydrothermal growth. Similar spatial variation in the TL and OSL in quartz was reported by Hashimoto *et al.* (1997) who attributed the striped patterns to the anisotropy of impurity distribution. Such data suggest that in the

case of sedimentary quartz, the cause of significant variability of the OSL intensity of single grains is related to growth conditions of the progenitor single crystals, although the effects of heat treatment is a further factor to take into account in the case of quartz extracted from heated materials.

3.2. Dose reconstruction

Having established the feasibility of obtaining an OSL map and measuring OSL decay curves at specific locations in sliced ceramic, the spatially-resolved determination of absorbed dose was investigated. This was performed with slices in two stages by: i) scanning, using low power and short duration stimulation, to produce an OSL map and identify the location of 'spots' emitting sufficient luminescence; ii) application of a regeneration procedure to determine the absorbed dose at the spots identified in the mapping. The loss of trapped charge due to depletion during the mapping process was corrected using of the form of the decay curve measured in the second stage and taking into account the differences in the intensity of the stimulation beam. In samples tested so far, the correction for depletion due to the scanning procedure is in the range 5-7%, but this is likely to vary between types of ceramic sample. The reliability of this correction was tested by administering a beta dose of 350 mGy to an optically bleached slice, performing a scan to obtain the OSL map, and then determining the 'recovered' dose using a regenerative procedure at the known luminescent spot(s). The recovered value of absorbed dose was 325±35 mGy which corresponds to an average depletion of 7% due to the scan procedure, and this agrees well with the estimate of 6±1 % based on examination of the form of the OSL decay curve for the measurement location.

The dose evaluation procedure was tested with slices cut from a 28 year-old brick that had been obtained from a Russian settlement contaminated by Chernobyl fallout. A sample from

the same brick had been previously examined in detail to obtain absorbed dose determinations with separated coarse grains (Bailiff *et al.*, 2000, 2002b). Since no acid etching treatments were applied to the cut surface, any grains exposed by the cutting process retained an alpha dose contribution. Subsequent inspection under a microscope indicated that the exposed grains were generally free of coatings, although other types of ceramic may require some form of cleaning treatment to improve the brightness of the luminescence.

OSL maps for slices were obtained and the location of spots exhibiting sufficiently bright luminescence identified; a representative example is given in Fig. 8. In a subsequent experiment, the OSL from these areas was confirmed to be due to quartz by examination of the time-resolved luminescence spectrum (see below). Using a regenerative procedure, values of absorbed dose of 334±34, 357±27 and 330±22 mGy were obtained (uncertainties are precision only) for the three different spots indicated, yielding an average value of 340±15 mGy (s.d. 3). An upper limit of 15 mGy was estimated for the alpha dose contribution using typical parameter values (a=0.1; 125 μm grain dia.; 20 μm penetration) and measured dose-rates. After subtraction of the alpha dose contribution, the *in-situ* grain result is encouragingly close to the consensus value of 325±15 mGy obtained using a multiple-grain procedure with quartz extracted from the equivalent depth range in the same brick (Bailiff *et al.*, 2002b). The close agreement in this case may be fortuitous given the precision obtained using a simplified regeneration procedure, but it nonetheless points to the feasibility of the *in-situ* grain approach with sliced ceramics, albeit with their sparse occurrence in the particular samples tested.

3.3. Time resolved measurement

Although, as discussed above, an indication of mineral type can be inferred by the form of the OSL decay curve or by stimulation with IR radiation (to identify feldspars), it can also be

obtained by examination of the TRL spectrum. Whereas the TRL associated with quartz and detected in the UV region is dominated by a decay component with a lifetime of 30-40 μs (Bailiff, 2000), different types of feldspars exhibit complex decay spectra that have component lifetimes of less than 1 μs (Clark *et al.*, 1997; Clark and Bailiff, 1998) and this difference provides a means of differentiating the two mineral species.

This approach was used to investigate the mineral composition of brick that had been collected from the Chernobyl and Semipalatinsk regions. Powder XRD spectra indicated that the former contained predominantly quartz and the latter a mixture of quartz and feldspar. A slice of the brick from the Semipalatinsk region was first scanned using 850 nm pulsed radiation and the OSL map, obtained by measuring the integrated luminescence, contains several distinctive spots of emission (labelled A-C), as shown in Fig. 9a. The TRL spectra obtained at these locations (Fig. 10) are characteristic of feldspathic minerals, having a dominant decay component with a lifetime in the range 2- 5 μs (Clark *et al.*, 1997). The OSL map obtained after a second scan, performed using 500 nm stimulation; and shown in Fig 9b includes spots A and B identified under 850 nm stimulation and an additional strongly emitting spot D. The TRL spectra for locations A and B were similar in form (the intensity was reduced during the second scan); analysis of the spectrum recorded at location B (Fig 9b) indicates two lifetime components of ~ 0.5 μs (dominant) and ~2 μs and this is consistent with the behaviour observed with potassic feldspars when stimulating with IR and changing the detection window from broad band to the UV (Clark and Bailiff, 1998). This evidence, combined with the measurement of TRL under both IR and visible stimulation at the same location, strongly suggests that the emitting minerals are feldspathic. Several new brightly emitting spots were also resolved under green stimulation and their TRL spectra were found to be characteristic of quartz (dominated single component with mean lifetime ~33 μs), as

shown by the TRL spectrum recorded at location D (Fig. 11) and is quite distinct from that measured at location B, attributed to a feldspathic mineral. The slices of brick from the Chernobyl region that were the subject of the absorbed dose measurements discussed above were also examined using this approach and the areas used for absorbed dose determination were confirmed to be quartz on the basis of their TRL spectra.

Although confirmation of the mineral type (e.g. thin section or electron probe measurements) or detailed examination of the TRL spectra has not been attempted here, these results illustrate the potential of the method for differentiating mineral components. While the ceramics examined here are relatively simple in composition, this approach is a potentially powerful means of mapping the distribution of coarse grains of different mineral types. Moreover, if the stimulation source was confined to visible wavelengths only, it is possible to map both quartz and feldspar distribution by using a pulsed stimulation source and analysing the data in the time domain.

4. Conclusions

The results described in this paper demonstrate the capability of a scanning technique to perform mapping of OSL from minerals located in the exposed surface of cut specimens and to selectively stimulate areas to produce OSL decay curves. The ability to determine the absorbed dose within a selected area of a ceramic surface provides an important advance for use in retrospective dosimetry. While on one hand the occurrence of a small number of luminescing areas is a disadvantage in terms of spatial resolution of absorbed dose determinations, the brightness of the luminescing areas in the brick types tested allowed the measurement of absorbed doses as low as ~0.1 Gy in ‘spot’ locations. When combined with pulsed laser stimulation and a time-resolved detection technique, the system has the capability

to differentiate between feldspar and quartz in mixed mineral samples using a single (visible) stimulation wavelength. On the basis of previous TRL studies more sophisticated mineral identification may be possible. Given the recent availability of compact pulsed laser sources and luminescence readers able to measure single grain ,wider access to measurements of this type is now feasible.

Acknowledgements

The work described in this paper was supported by the University of Durham and the European Commission within its 5th Framework Programme (1998-2002), Nuclear Fission and Radiation Protection, under Contract N° FIGD-CT-2000-00094. The latter is a collaborative project with: Ciemat, Madrid, GSF Neuherberg, Risø National Laboratory and the University of Helsinki. Earlier financial support by the NERC (grantss GR3/9568 and GST/02/0756) for development of a prototype scanning system is also acknowledged. We are grateful to Dr. R. Clark for programming, Dr. S. Chyriwsky for assistance in developing the prototype scanner and Mr. S. Grainger for technical assistance in sample preparation. We are grateful to Landauer Inc. for donation of Al_2O_3:C dosemeter powder.

References

Attix, F.H., 1986. Introduction to Radiological Physics and Radiation Dosimetry. Wiley Interscience Publication, New York.

Bailiff, I.K., Clark, R.J., Barnett, S.M., 1996. A high resolution scanning system for measurement spatially resolved optically stimulated luminescence. Abstract of 8th International Conference on Luminescence and Electron Spin Resonance Dating, Canberra Australia.

Bailiff, I.K., 2000. Characteristics of time-resolved luminescence in quartz. Radiation Measurements 32, 401-405.

Bailiff, I.K., Bøtter-Jensen, L., Correcher, V., Delgado, A., Göksu, H.Y., Jungner, H., Petrov, S., 2000. Absorbed dose evaluations in retrospective dosimetry: methodological developments using quartz. Radiation Measurements 32, 609-613.

Bailiff, I.K., Correcher, V., Delgado, A., Göksu, Y., Hübner, S., 2002a. Luminescence characteristics of dental ceramic for retrospective dosimetry – a preliminary study. Radiation Protection Dosimetry 101, 519-524.

Bailiff, I.K., Stepanenko, V.F., Göksu, H.Y. Balonov, M., Bøtter-Jensen, L., Chumak, V., Correcher, V., Delgado, A., Golikov, S., Jungner, H., Likhtarev, I. Khamidova, L.G. Kolizshenkov T.V., Meckbach, R., Petrov, S.A., Sholom, S., 2002b. Comparison of retrospective luminescence dosimetry with computational modelling in two highly contaminated settlements downwind of the Chernobyl NPP. Health Physics (submitted).

Blasse, G., Grabmaier, B.C., 1994. Luminescent Materials. Springer-Verlag, Berlin, Heidelberg.

Bøtter-Jensen, L., Jungner, H., Poolton, N.R.J., 1995. A continuous OSL scanning method for analysis of radiation depth-dose profiles in bricks. Radiation Measurements 24, 525-529.

Clark, R.J., Bailiff, I.K., Tooley, M.J., 1997. A preliminary study of time-resolved luminescence in some feldspars. Radiation Measurements 27, 211-220.

Clark, R.J., Bailiff, I.K., 1998 Fast time-resolved luminescence emission spectroscopy in some feldspars. Radiation Measurements 29, 553-560.

Duller, G.A.T, Bøtter-Jensen, L., Markey, B.G., 1997. A luminescence imaging system based on a charge coupled device (CCD) camera. Radiation Measurements 27, 91-99.

Duller, G.A.T, Bøtter-Jensen, L., Kohsiek, P., Murray, A.S., 1999. A high-sensitivity optically stimulated luminescence scanning system for measurement of single sand-sized grains. Radiation Protection Dosimetry 84, 325-330.

Duller, G.A.T, Bøtter-Jensen, L., Murray, A.S., 2000. Optical dating of single sand-sized grains of quartz: sources of variability. Radiation Measurements 32, 453-457.

Göksu, H.Y., Bailiff, I.K., Mikhailik, V.B., 2002. New approaches to retrospective dosimetry using cementitious building materials. Radiation Measurements (submitted for publication).

Göksu, H.Y., Bailiff, I.K., Bøtter–Jensen, L., Hutt, G., 1995. Interlaboratory beta source calibration using TL and OSL on natural quartz. Radiation Measurements 24, 479-483.

Greilich, S., Glasmacher, U.A., Wagner, G.A., 2002. Spatially resolved detection of luminescence – a unique tool for archaeochronometry. Naturwissenschaften 89, 371-375.

International Commission on Radiation Units and Measurements, 1984. Stopping Powers for Electrons and Positrons. ICRU Report 37.

Hashimoto, T., Yokosaka, K., Hubuki, H., Hayashi, Y., 1989. Provenance search of dune sands using thermoluminescence colour images (TLCIs) from quartz grains. Radiation Measurements 16, 3-10.

Hashimoto, T., Notoya, S. Ojima T., Hoteida, M., 1995. Optically stimulated luminescence (OSL) and some other luminescence images from granite slices exposed with radiations, Radiation Measurements 24, 227-237.

Hashimoto, T., Katayama, H., Sakaue, H., Hase, H., Arimura, T., Ojima, T., 1997. Dependence of some radiation induced phenomena from natural quartz on hydroxyl-impurity contents. Radiation Measurements 27, 243-250.

Huntley, D.J., Kirkey, J.J., 1985. The use of an image intensifier to study the TL intensity variability of individual grains. Ancient TL 3, 1-4.

McFee, C.J., Tite, M.S., 1994. Investigations into the thermoluminescence properties of single quartz grains using an imaging photon detector. Radiation Measurements 23, 355-360.

McKeever, S.W.S., Bøtter-Jensen, L., Agersnap Larsen, N., Duller, G.A.T., 1997. Temperature dependence of OSL decay curves: experimental and theoretical aspects. Radiation Measurements 27, 161-170.

Petrov, S.A., Bailiff, I.K., 1995. The '110°C' peak in synthetic quartz. Radiation Measurements 24, 519-523.

Poolton, N.R.J., Bøtter-Jensen, L., Jungner, H., 1995. An optically stimulated luminescence study of porcelain related to radiation dosimetry. Radiation Measurements 24, 543-549.

Smith, B.W., Wheeler, G.C.W.S., Rhodes, E.J., Spooner N.A., 1991. Luminescence dating of zircon using an imaging photon detector. Nuclear Tracks and Radiation Measurements 18, 273-278.

Spooner, N.A., 2000. A photon-counting imaging system (PCIS) for luminescence applications. Radiation Measurements 32, 513-521.

Spooner, N.A., Allsop, A., 2000. The spatial variation of dose rate from $^{90}Sr/^{90}Y$ beta sources for use in luminescence dating. Radiation Measurements 32, 49-56.

Templer, R., Walton, A., 1983. Image intensifier studies of TL in zircons. PACT 9, 299-308.

Thoms, M., von Seggern, H., 1996. Radiographic imaging with image plates: The influence of the readout intensity on the image quality. Journal of Applied Physics 81, 5887-5895.

I.K.Bailiff and V.B.Mikhailik Spatially-resolved measurement of optically stimulated luminescence and time-resolved luminescence

Figure captions

Fig.1. Schematic representation of high-resolution scanning system for measurement of spatially-resolved optically stimulated luminescence.

Fig.2. OSL map from a slice of brick collected from the Chernobyl region and decay curves measured for specified spots (insets). The density scale represents the intensity of the OSL signal detected for the image pixel.

Fig.3. OSL map from a concrete slice and the decay curves measured for the specified spots (a and b).

Fig.4. OSL maps of dental porcelain slices. Insets show OSL decay curves for specified spots. Laboratory dose is 8 Gy.

Fig.5. OSL map of a porcelain slice (cut perpendicular to the surface) and the OSL signal profile. Laboratory dose is 3 Gy.

Fig. 6. OSL map of a 1 mm thick Al_2O_3:C slice (cut perpendicular to irradiated surface) and average profile of OSL intensity. Laboratory irradiation performed with a beta source (sub surface dose ~ 0.8 Gy) was in the direction indicated by arrow. The step interval used was 100 μm.

Figure 7. Isometric (a) and contour (b) OSL intensity maps obtained with a slice of single crystal quartz (Sawyer Premium 'Q'). The sample was annealed at 1000°C and the dose administered was 2 Gy. The outermost contour line shown in b) corresponds well with the physical shape of the sample.

Figure 8. OSL map of a brick slice and regenerative growth curves obtained for the specified spots (A-C). The accrued dose was estimated to be: 334±34 (A), 357±27 (B) and 330±22 mGy (C). Preheat to 200ºC at $2^{o}s^{-1}$.

Figure 9. OSL maps of a brick slice (Semipalatinsk) obtained using pulsed laser stimulation: (a) stimulation 850 nm (detection filter, BG-39), (b) stimulation 500 nm (detection filter, U-340); the incremental step used was 400 μm. The laboratory dose administered was ~70 Gy.

Figure 10. TRL spectra recorded for specified spots on the brick surface (see Fig. 9) using pulsed infrared stimulation (850 nm) and BG-39 optical filter. Solid lines represent two-exponential fitting to the experimental data: A-τ_1=1.5 μs, τ_2=9.4 μs; B-τ_1=2.0 μs, τ_2=6.1 μs; C- τ_1=1.4 μs, τ_2=7.6 μs.

Figure 11. TRL spectra recorded for specified spots of the brick surface (see Fig. 9) using pulsed 500 nm stimulation (detection filter, U-340). Solid lines represent exponential fitting to the experimental data: D- τ_1=33 μs, B- τ_1=0.5 μs, τ_2=2.1 μs.

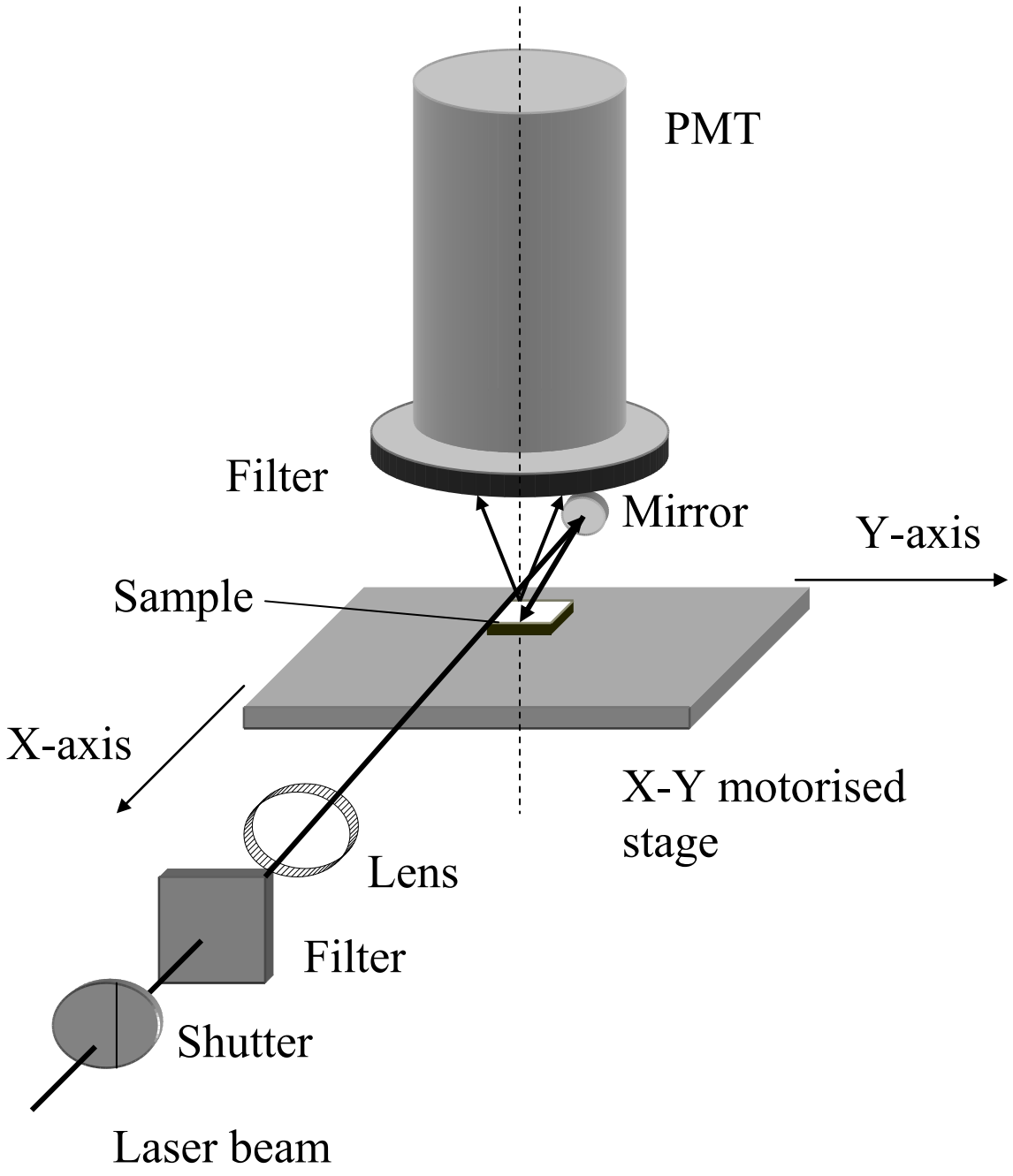
PMT
Filter
Mirror
Y-axis
Sample
X-axis
X-Y motorised stage
Lens
Filter
Shutter
Laser beam

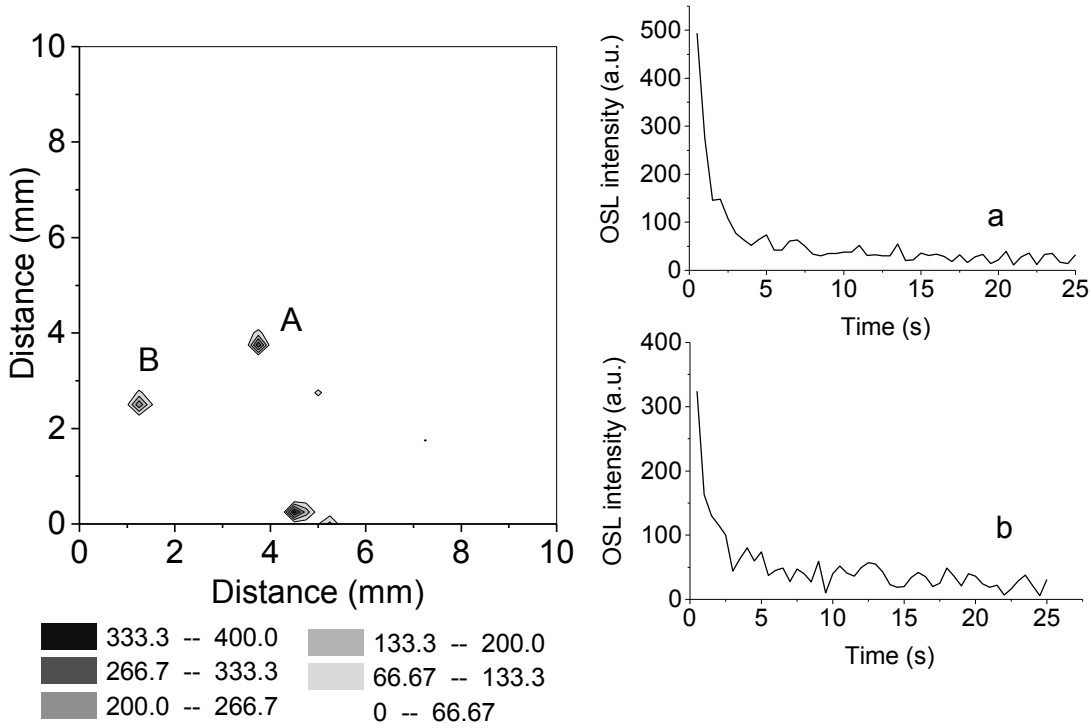
Distance (mm)
Distance (mm)
A
B
333.3 -- 400.0
266.7 -- 333.3
200.0 -- 266.7
133.3 -- 200.0
66.67 -- 133.3
0 -- 66.67
OSL intensity (a.u.)
Time (s)
a
OSL intensity (a.u.)
Time (s)
b

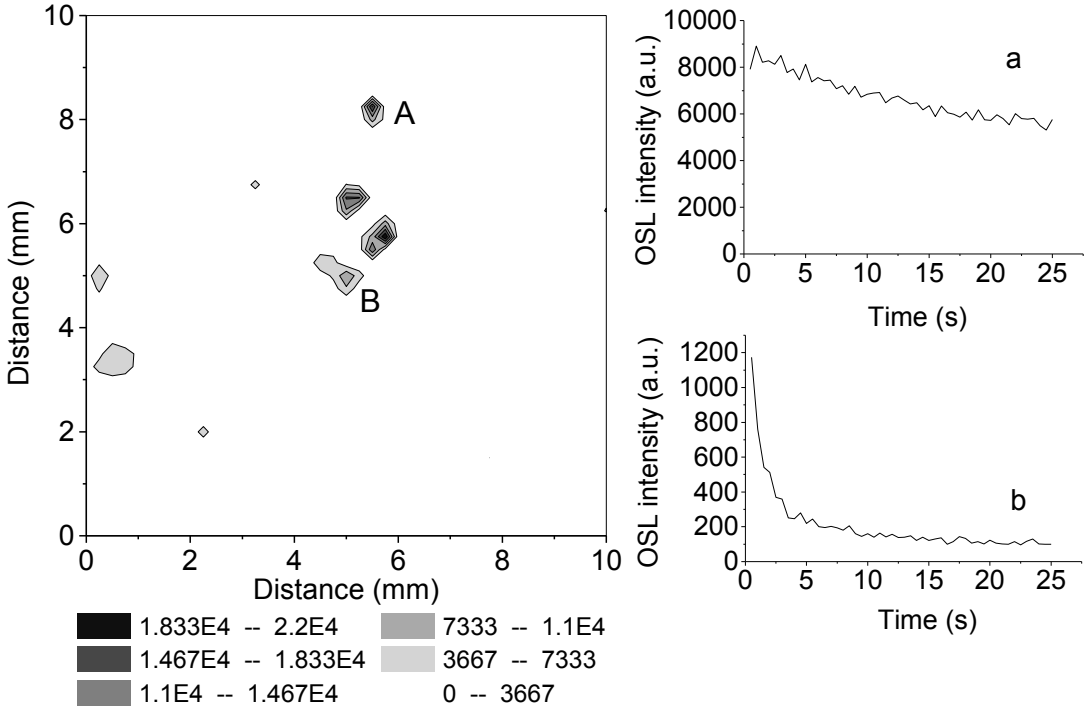
Distance (mm)
Distance (mm)
A
B
1.833E4 -- 2.2E4
1.467E4 -- 1.833E4
1.1E4 -- 1.467E4
7333 -- 1.1E4
3667 -- 7333
0 -- 3667
OSL intensity (a.u.)
Time (s)
a
OSL intensity (a.u.)
Time (s)
b

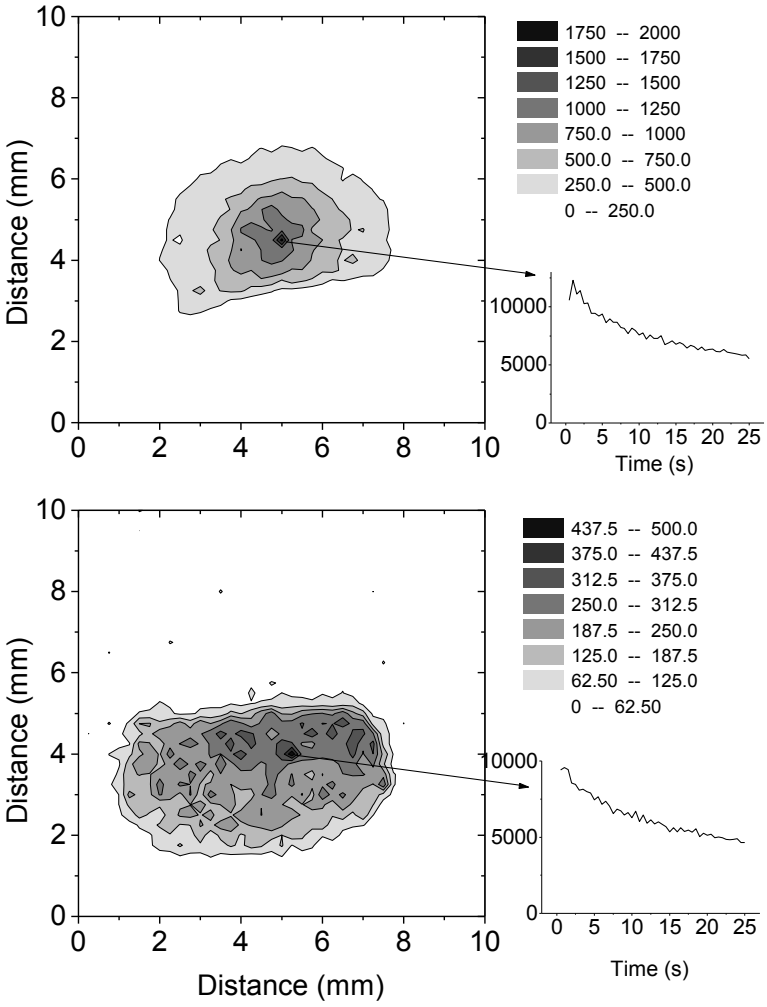
Distance (mm)
Distance (mm)
1750 -- 2000
1500 -- 1750
1250 -- 1500
1000 -- 1250
750.0 -- 1000
500.0 -- 750.0
250.0 -- 500.0
0 -- 250.0
437.5 -- 500.0
375.0 -- 437.5
312.5 -- 375.0
250.0 -- 312.5
187.5 -- 250.0
125.0 -- 187.5
62.50 -- 125.0
0 -- 62.50
Time (s)
Time (s)

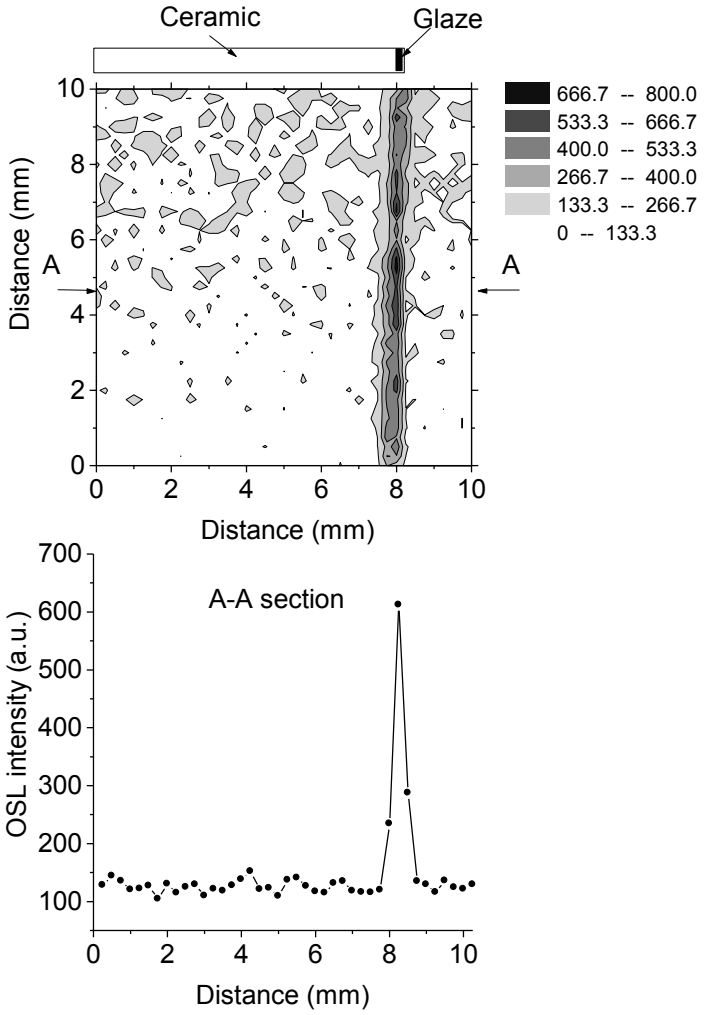
Ceramic
Glaze
666.7 -- 800.0
533.3 -- 666.7
400.0 -- 533.3
266.7 -- 400.0
133.3 -- 266.7
0 -- 133.3
Distance (mm)
A
A
Distance (mm)
A-A section
OSL intensity (a.u.)
Distance (mm)

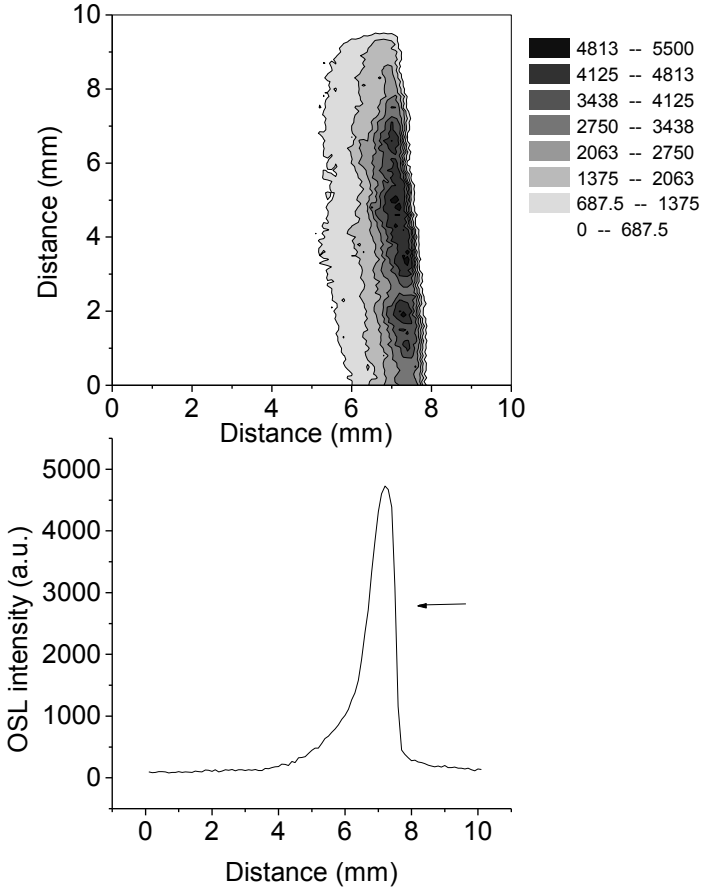
4813 -- 5500
4125 -- 4813
3438 -- 4125
2750 -- 3438
2063 -- 2750
1375 -- 2063
687.5 -- 1375
0 -- 687.5
Distance (mm)
Distance (mm)
OSL intensity (a.u.)
Distance (mm)

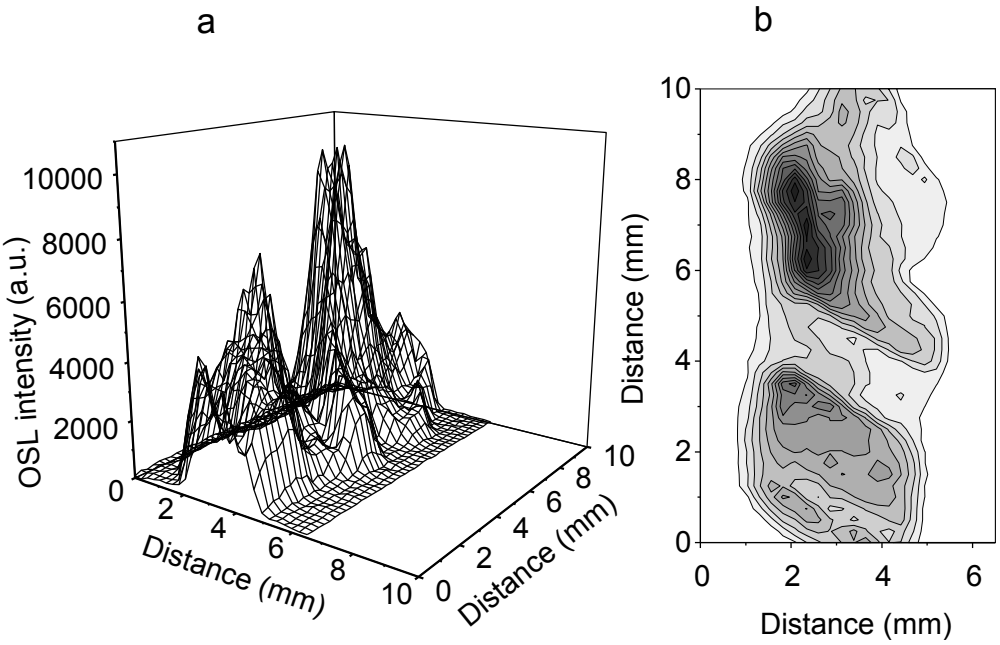
a
b
OSL intensity (a.u.)
10000
8000
6000
4000
2000
0
Distance (mm)
Distance (mm)
Distance (mm)
Distance (mm)
0
2
4
6
8
10

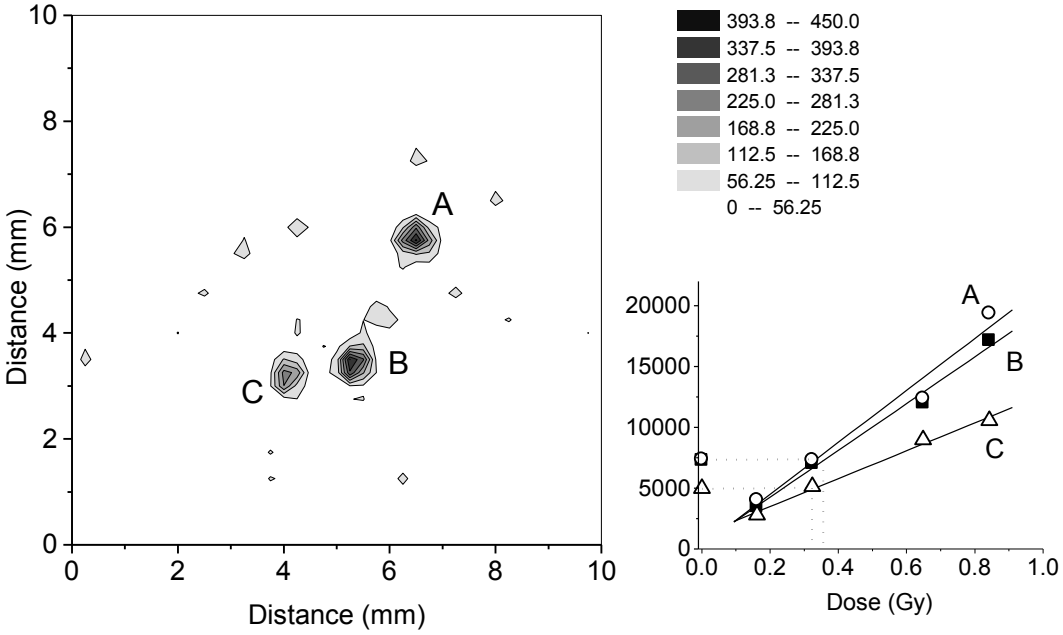
393.8 -- 450.0
337.5 -- 393.8
281.3 -- 337.5
225.0 -- 281.3
168.8 -- 225.0
112.5 -- 168.8
56.25 -- 112.5
0 -- 56.25
Distance (mm)
Distance (mm)
A
B
C
Dose (Gy)

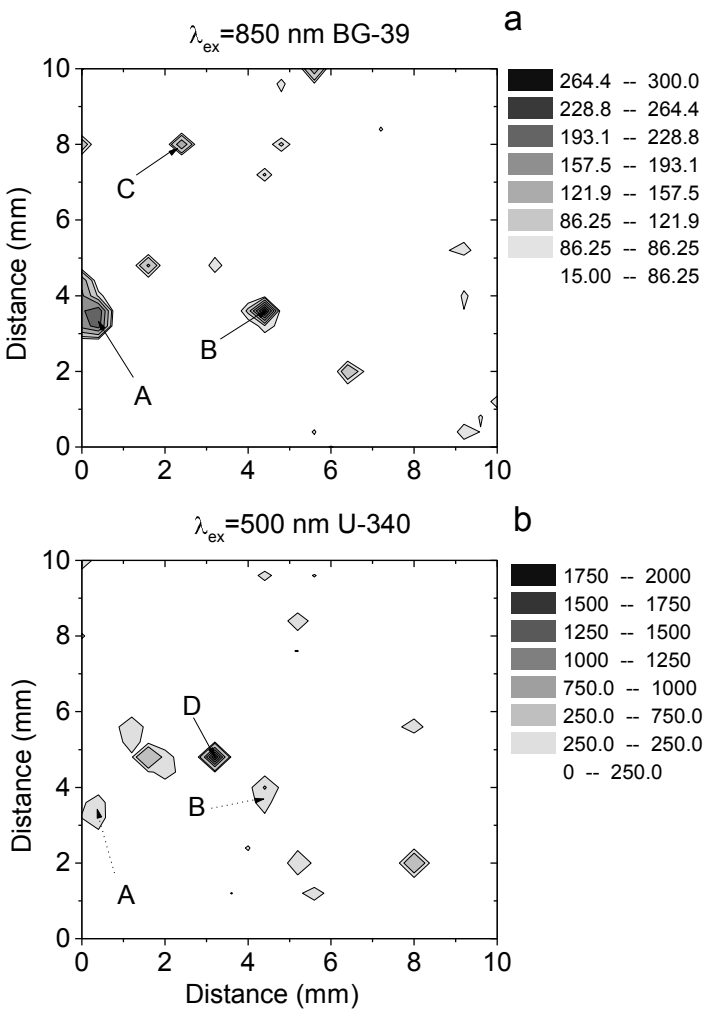
a
λex=850 nm BG-39
Distance (mm)
C
B
A
264.4 -- 300.0
228.8 -- 264.4
193.1 -- 228.8
157.5 -- 193.1
121.9 -- 157.5
86.25 -- 121.9
86.25 -- 86.25
15.00 -- 86.25
b
λex=500 nm U-340
Distance (mm)
D
B
A
1750 -- 2000
1500 -- 1750
1250 -- 1500
1000 -- 1250
750.0 -- 1000
250.0 -- 750.0
250.0 -- 250.0
0 -- 250.0

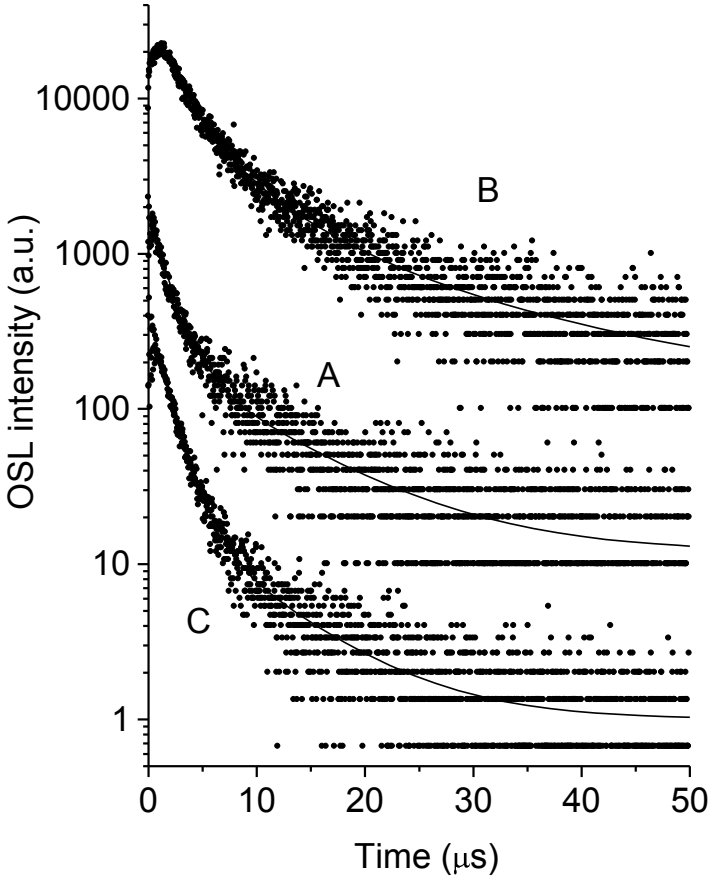
OSL intensity (a.u.)
10000
1000
100
10
1
0
10
20
30
40
50
Time (μs)
A
B
C

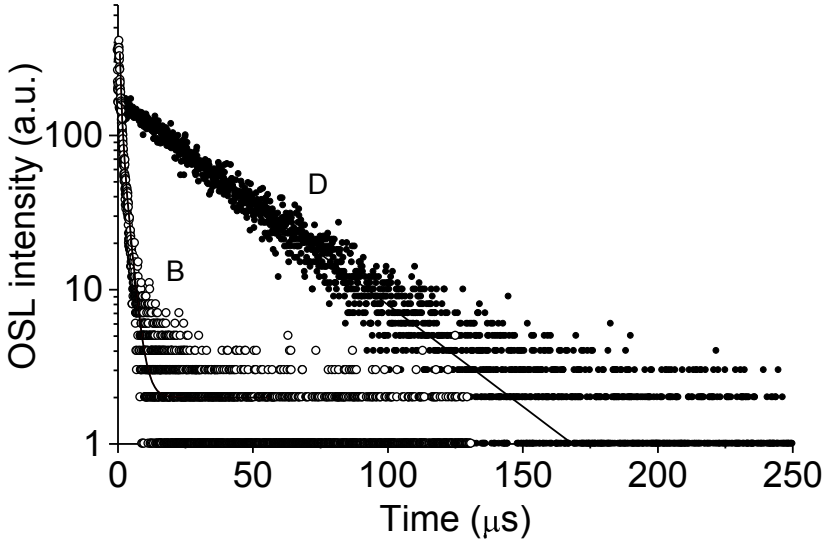
OSL intensity (a.u.)
100
10
1
0
50
100
150
200
250
Time (μs)
D
B